

Numerical Simulation of Two-Phase Flow and Solute Transport During Microbial Enhanced Oil Recovery

J. Li¹, J. Liu¹, M.G. Trefry^{2,3}, J. Park², K. Liu⁴, B. Haq¹,
C.D. Johnston^{2,3}, B. Clennell⁴ and H. Volk⁴

¹School of Mechanical Engineering

The University of Western Australia, Perth, Western Australia 6009, Australia

²CSIRO Land and Water, Private Bag No.5, Wembley, Western Australia 6913, Australia

³School of Earth and Environment

The University of Western Australia, Perth, Western Australia 6009, Australia

⁴CSIRO Petroleum Resources, PO Box 136, North Ryde, New South Wales 1670, Australia

Abstract

Microbial enhanced oil recovery (MEOR) is a potential low cost method for increasing crude oil recovery. Before MEOR field applications can be performed with confidence, it is important to understand key mechanisms and quantitative relationships between microbial metabolism, permeability, interfacial tension and residual oil saturation. In this study, a fully coupled finite element model of the MEOR processes in homogeneous and heterogeneous porous media is presented. This model includes biological and hydrological processes and also describes how the interfacial tension reduces the residual oil saturation. Numerical simulations of core flooding experiments are performed to investigate the influence of different bacterial concentrations and types on the oil recovery. Results show that the microbial processes in homogeneous porous media can increase the oil recovery significantly if water containing suitable bacterial concentration and type is injected. Simulations using a sandstone porosity distribution measured via X-ray CT show that the heterogeneity of the rock has a significant effect on the MEOR processes.

Introduction

MEOR has been studied through laboratory experiments, field applications and numerical simulations. Mathematical models for microbial enhanced oil recovery have been developed in reservoir engineering since 1990. Islam [4] investigated microbial transport and nutrient propagation in multidimensional porous media. In that model, dispersion and diffusion were neglected. Chang *et al.* [3] proposed a one-dimensional model with a nonlinear equation which described the growth and decay of microbes on the rock surface, including bulk clogging and declogging effects. Another one-dimensional model was developed by Zhang *et al.* [10]. In that work, the conservation equation for the sessile phase included biomass retention, detachment and growth. In many previous MEOR modelling studies the residual oil saturation has been assumed to be a constant. This assumption is inconsistent with the MEOR objective. Recently, Li *et al.* [6] developed a fully coupled biological (B) and hydrological (H) finite element model that introduced a modification to the residual oil saturation under several assumptions.

MEOR laboratory studies and field applications were reported over the past two decades. Karim *et al.* [5] discussed the results of microbial treatment in the Bokor field, Malaysia. They found that treated wells increased oil production and reduced water-cut

significantly over a five month period. Further works [7] regarding laboratory tests and fields applications of the MEOR technique were carried out in the Daqing oilfield in China. The results showed that MEOR was suitable and attractive for the Daqing oilfield.

In this study, the coupled BH model is applied to a 2-D numerical experiment to investigate the influence of different model bacterial concentrations and types on the oil recovery. Further, it is extended to include rock heterogeneity as characterized by a non-destructive imaging technique (X-ray CT scan). The numerical results show that MEOR in homogeneous porous media increases the oil recovery significantly if water containing suitable bacterial concentration and type is injected. For heterogeneous systems, variations in flow and transport distributions significantly alter MEOR performance.

Governing Equations of Two-Phase Flow

The flow equations describing two-phase flow in porous media are

$$\frac{\partial(\phi S_w)}{\partial t} + q_w = \nabla \cdot \left[\frac{KK_{r,w}}{\mu_w} \nabla(p_w - \rho_w gh) \right], \quad (1)$$

$$\frac{\partial(\phi S_o)}{\partial t} + q_o = \nabla \cdot \left[\frac{KK_{r,o}}{\mu_o} \nabla(p_o - \rho_o gh) \right], \quad (2)$$

$$S_w + S_o = 1, \quad (3)$$

$$p_c(S_w) = p_o - p_w, \quad (4)$$

where ϕ is the porosity, ρ_l is the fluid density of phase l ($l = w$ for water or $l = o$ for oil), μ_l is the fluid viscosity, S_l is the saturation, p_l and p_c are the pressure and the oil-water capillary pressure, respectively. K and $K_{r,l}$ denote the absolute and relative permeabilities, q_l is the source/sink term, g is the gravitational acceleration and h is the distance. The capillary pressure is a function of the saturation S_w which may be given by different models.

Governing Equations of Solute Transport

The transport equations for the bacteria, nutrients and metabolic products in the water phase are written as

$$\frac{\partial(\phi S_w C_b)}{\partial t} = \nabla \cdot (\phi S_w \bar{D}_b \nabla C_b) - \nabla \cdot (u_w C_b + \phi V_g C_b) + R_b, \quad (5)$$

$$\frac{\partial(\phi S_w C_n)}{\partial t} = \nabla \cdot (\phi S_w \bar{D}_n \nabla C_n) - \nabla \cdot (u_w C_n) + R_n, \quad (6)$$

$$\frac{\partial(\phi S_w C_p)}{\partial t} = \nabla \cdot (\phi S_w \bar{D}_p \nabla C_p) - \nabla \cdot (u_w C_p) + R_p, \quad (7)$$

where C_b, C_n and C_p are the concentrations of bacteria, nutrients and metabolic products, respectively; \bar{D}_b, \bar{D}_n and \bar{D}_p are dispersion tensors for bacteria, nutrients and metabolic products, u_w is the Darcy flux vector for the water phase and V_g is the settling velocity of bacteria; the reaction rates (R_b, R_n, R_p) are given by

$$R_b = -k_1 \phi S_w C_b + k_2 \rho_b \sigma_1 - k_3 \phi S_w C_b + g_1 \phi S_w C_b - d_1 \phi S_w C_b - \frac{R_p}{Y_{p/b}}, \quad (8)$$

$$R_n = -\frac{R_p}{Y_{p/s}} - Y_s (\phi S_w C_b + \rho_b \sigma), \quad (9)$$

$$R_p = \mu_{p,max} \frac{C_n - C_s^*}{K_{p/s} + C_n - C_s^*} (\phi S_w C_b + \rho_b \sigma). \quad (10)$$

In the above expressions, k_1 is the reversible bacterial attachment rate, k_2 is the bacterial detachment rate, k_3 is the irreversible bacterial attachment rate, g_1 is the bacterial growth rate, d_1 is the bacterial decay rate, ρ_b is the density of bacteria, $\sigma = \sigma_1 + \sigma_2$ is the total volumetric fraction of bacteria attached where σ_1 and σ_2 are the volumetric fractions of bacteria attached reversibly and irreversibly; $Y_{p/b}$ is the bio-product yield coefficient per unit bacteria, $Y_{p/s}$ is the bio-product yield coefficient per unit nutrient, Y_s is the yield coefficient representing nutrient consumed, $\mu_{p,max}$ is the maximum specific production rate, $K_{p/s}$ is the saturation constant for production of product by consuming nutrient, and C_s^* is the critical nutrient concentration for metabolism. The bacterial growth rate (g_1) depends on the nutrient concentration, and is defined by a Monod type of growth rate

$$g_1 = g_{1,max} \frac{C_n}{K_{b/s} + C_n}, \quad (11)$$

where $g_{1,max}$ is the maximum growth rate and $K_{b/s}$ is the saturation constant, at which concentration the specific growth rate reaches half of its maximum value.

The mass balance equations for bacteria deposited reversibly and irreversibly are written as

$$\frac{\partial(\rho_b \sigma_1)}{\partial t} = k_1 (\phi_0 - \sigma) C_b - k_2 \rho_b \sigma_1 + g_1 \rho_b \sigma_1 - d_1 \rho_b \sigma_1, \quad (12)$$

$$\frac{\partial(\rho_b \sigma_2)}{\partial t} = k_3 (\phi_0 - \sigma) C_b + g_1 \rho_b \sigma_2 - d_1 \rho_b \sigma_2, \quad (13)$$

where ϕ_0 is the initial porosity. The porosity reduction caused by bacterial attachment is defined as follows

$$\phi = \phi_0 - \sigma = \phi_0 - \sigma_1 - \sigma_2 \geq 0. \quad (14)$$

The porosity reduction is quantified by solving equations (12) and (13) at each time step. The relation between the permeability and the biomass-modified porosity is defined by

$$K = K_0 \left(\frac{\phi}{\phi_0} \right)^{19/6}, \quad (15)$$

where K_0 is the initial absolute permeability. The dispersion tensors, the capillary pressure model and the relative permeability formula are defined as in [6].

Interfacial Tension and Residual Oil Saturation

The metabolic products include bio-surfactants, polymers and other compounds. In this study, we suppose that the ratio of the bio-surfactant to the total metabolic products is given as follows

$$a_{ps} = \frac{C_{ps}}{C_p}, \quad 0 \leq a_{ps} < 1, \quad (16)$$

where C_{ps} is the surfactant concentration. Surfactants reduce the interfacial tension between the oil and water phases which is one of the most important mechanisms for increasing oil recovery.

An interfacial tension model describing the relationship between interfacial tension and surfactant concentration was developed by Bang and Caudle [2]. We use their formula to construct the following model

$$\sigma_{Int}(t + \Delta t) = \min \left\{ \sigma_{Int}(t), \sigma_{Int,\min} \left(\frac{\sigma_{Int,\max}}{\sigma_{Int,\min}} \right)^{\left(\frac{C_{ps,\max} - \bar{C}_{ps}}{C_{ps,\max} - C_{ps,\min}} \right)^s} \right\} \quad (17)$$

where σ_{Int} , $\sigma_{Int,\min}$ and $\sigma_{Int,\max}$ are the interfacial tension and its minimum and maximum, $C_{ps,\min}$ and $C_{ps,\max}$ are the surfactant concentration's minimum and maximum, \bar{C}_{ps} is the average surfactant concentration, s is an exponent parameter. This means that the interfacial tension decreases from its maximum to minimum as the surfactant concentration increases.

The dimensionless total trapping number which quantifies the force balance on oil in porous media was introduced by Pennell *et al.* [9]. The trapping number is defined by the following

$$N_T = \sqrt{N_{Ca}^2 + 2N_{Ca}N_B \sin \alpha_0 + N_B^2}, \quad (18)$$

where α_0 is the angle of flow relative to the horizontal; N_{Ca} is the capillary number and N_B is the Bond number, which are defined as

$$N_{Ca} = \frac{u_w \mu_w}{\sigma_{int} \cos \theta} \quad \text{and} \quad N_B = \frac{\Delta \rho g K K_{r,w}}{\sigma_{int} \cos \theta}, \quad (19)$$

where u_w is the Darcy flux of the aqueous phase, μ_w is the viscosity of the aqueous phase, θ is the contact angle between the aqueous/non-aqueous interface and the porous medium, $\Delta \rho$ is the density difference between the aqueous and non-aqueous phases.

A functional relation between the trapping number and the residual oil saturation is presented by Li *et al.* [8]. Based on this relation, the residual oil saturation is defined as follows

$$S_{or}(t + \Delta t) = \min \left\{ S_{or}(t), S_{or}^{\min} + (S_{or}^{\max} - S_{or}^{\min}) \left[1 + (T_1 N_T)^{T_2} \right]^{1/T_2 - 1} \right\}, \quad (20)$$

where T_1 and T_2 are fitting parameters.

The details solving this coupled BH finite element model were given by Li *et al.* [6].

Results and Discussion

First, we test the model for homogeneous porous media. The computational domain is taken as the horizontal plane of a hypothetical core, (two-dimensional rectangular, length of 0.1 m, width of 0.02 m). The computational domain is divided into 2528 triangular elements. In our numerical example, the parameters are given in Table 1 (other parameters come from Table 2 in [6]) and the initial values for the pressures are given as follows

$$p_{w,0} = 0.1 \rho_w g \text{ Pa}, \quad (21)$$

$$p_{o,0} = 1.2 \rho_o g \text{ Pa}. \quad (22)$$

Parameter	Value	Parameter	Value
K_0	$0.14 \times 10^{-12} \text{ m}^2$	ϕ_0	0.28
$g_{1\max}$	$5 \times 10^{-6} \text{ s}^{-1}$	ρ_w	1000 kg m^{-3}
d_1	$1.0 \times 10^{-7} \text{ s}^{-1}$	ρ_o	800 kg m^{-3}
k_1	$2.28 \times 10^{-5} \text{ s}^{-1}$	ρ_b	1600 kg m^{-3}
k_2	$3.56 \times 10^{-7} \text{ s}^{-1}$	μ_w	$1.0 \times 10^{-3} \text{ kg m}^{-1} \text{ s}^{-1}$
k_3	$8.6 \times 10^{-6} \text{ s}^{-1}$	μ_o	$3.92 \times 10^{-3} \text{ kg m}^{-1} \text{ s}^{-1}$

Table 1. List of parameters for numerical experiments.

The nutrient concentration in the core is 0.5 before water injection. Assume that the Darcy flux at the inlet and outlet is 0.02 m/h and the injected bacterial concentration is 0.5. Three IFT-surfactant functions (17) are tested in our numerical experiments. They are denoted ‘‘bacteria’’ A, B and C. After bacteria A is injected, the interfacial tension decreases from 33.7 dyne/cm to 0.09 dyne/cm. If bacteria B or C is injected, the

interfacial tension decreases from 33.7 dyne/cm to 0.9 dyne/cm or from 33.7 dyne/cm to 9 dyne/cm, respectively. The minima of the residual oil saturation corresponding to the three bacterial models are different.

Figure 1 shows that the average interfacial tensions with the three bacteria injections reduce as the time increases. The least average interfacial tension is obtained by injecting bacteria A, while the effect of bacteria C yields least reduction of the average interfacial tension. Since the interfacial tension is an exponential function of the surfactant concentration, the interfacial tensions for all of three types of bacteria decrease dramatically in the first 0.8 hours as the surfactant concentrations increase. After 0.9 hour, the interfacial tensions reach their minima.

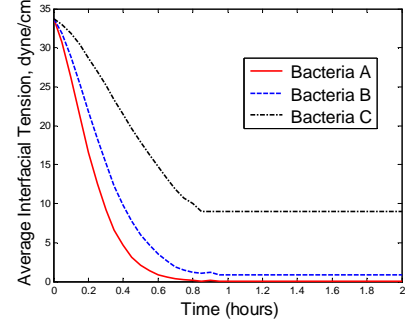


Figure 1. Comparison of the average interfacial tensions for three types of bacteria injections.

The residual oil saturation depends on the capillary number. Their relationship is shown by the capillary desaturation curve in Figure 2. Abrams [1] reports experimental results of short core flow tests which show the influence of interfacial tension. The average residual oil saturations obtained by the model are compared with experimental data [1] in Figure 2. It is observed that the capillary desaturation curve for bacteria A underestimates the measurements. It is possibly caused by unsuitable parameters values (T_1 and T_2) that come from the reference [8]. Since T_1 and T_2 are fitting parameters, their values may be adjusted to different cases so that numerical solution matches the experimental data. Figure 2 also shows that the capillary desaturation curves for bacteria B and C were better fitted to the experimental data for the ranges of their residual oil saturations (bacteria B: 0.17-0.3 and bacteria C: 0.2-0.3). That means that the estimates of the residual oil saturation minima for bacteria B and C were more reliable than the one for bacteria A.

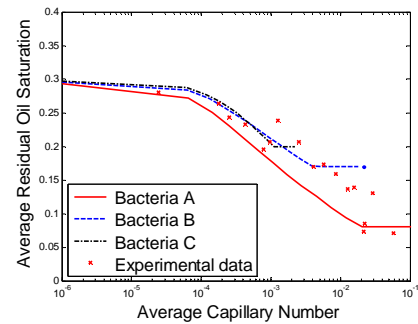


Figure 2. Comparison of the experimental data and simulations for three types of bacteria injections.

The comparison of the oil recoveries with three types of bacteria injections and without MEOR treatment is shown in Figure 3. In this example, it is observed that microbial metabolism increases the oil recoveries for bacteria A, B and C by 14%, 9% and 6%, respectively. This is because we used optimistic estimates of parameters in our computations. This example just demonstrates

the potential microbial effects on oil recovery and provides a mechanistic understanding of microbial enhanced oil recovery. Three different injected bacterial concentrations are tested but we only mention the results here. The higher the injected concentration is, the more the oil recovery increases. It means that the effect of the injected concentration on the oil recovery is significant.

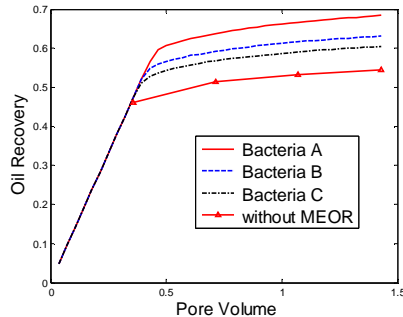


Figure 3. Comparison of the experimental data and simulations for three types of bacteria injections.

Second, we simulate the MEOR processes in a heterogeneous domain based on a X-ray CT image of a horizontal slice of sandstone. Assume that the horizontal slice's length and width are 0.1 m and 0.02 m respectively. The porosity in the 2-D rectangular domain is computed by transforming pixels of the X-ray CT image. Figure 4 shows the porosity distribution in the X-ray CT image. The mean porosity is 0.254.

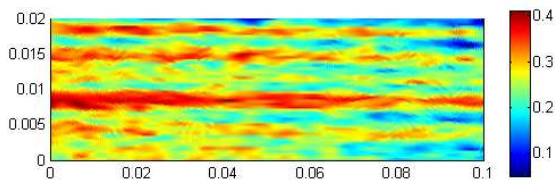


Figure 4. Porosity distribution in the X-ray CT image.

In our computations, the computational domain is divided into 2528 triangular elements and the time step is chosen automatically. All parameters, the initial and boundary conditions are taken from the homogeneous example. The simulated water content in the core slab at $t=0.5$ hour is shown in Figure 5. High porosity features admits large fluid fluxes. The arrows represent the water velocity.

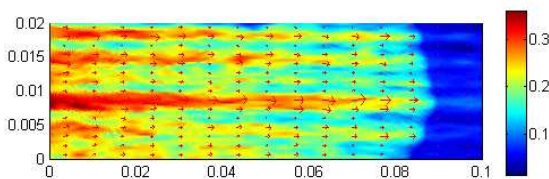


Figure 5. Simulated water content in the core slab at $t=0.5$ hour in a two-phase displacement simulation.

The bacterial concentration at $t=0.5$ hour is shown in Figure 6. It is observed that the heterogeneity has significant effects on the bacterial concentration although we did not give any comparison for homogeneous and heterogeneous porous media.

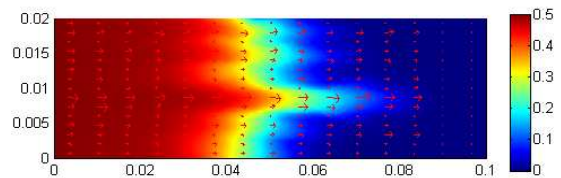


Figure 6. Simulated bacterial concentration in the core slab at $t=0.5$ hour.

Conclusions

A fully coupled biological and hydrological model is presented to simulate the microbial enhanced oil recovery processes in homogeneous and heterogeneous porous media. The effect of bacterial type on the interfacial tension and the oil recovery is significant. Different bacterial concentrations also affect the interfacial tension and the oil recovery. The heterogeneous property of the rock has a significant effect on flow and transport in the MEOR processes. Numerical results for the displacement experiment show that microbial metabolism in porous media may potentially increase the oil recovery significantly if water containing suitable bacterial concentration and type is injected.

Acknowledgments

This work was supported by WA:ERA and by CSIRO National Research Flagship Wealth from Oceans. The X-ray CT image of a horizontal slice of sandstone was provided by CSIRO Earth Science and Resource Engineering.

References

- [1] Abrams, A., The influence of fluid viscosity, interfacial tension, and flow velocity on residual oil saturation left by waterflood, *SPE J.*, **15**, 1975, 437-447.
- [2] Bang, H.W. & Caudle, B.H., Modeling of a micellar/polymer process, *SPE J.*, **24**, 1984, 617-627.
- [3] Chang, M-M., Chung, F.T-H., Bryant, R.S., Gao, H.W. & Burchfield, T.E., Modeling and laboratory investigation of microbial transport phenomena in porous media, *SPE*, **22845**, 1991, 299-308.
- [4] Islam, M.R., Mathematical modeling of microbial enhanced oil recovery, *SPE*, **20480**, 1990, 159-168.
- [5] Karim, M.G.A., Salim, M.A.H., Zain, Z.M. & Talib, N.N., Microbial enhanced oil recovery (MEOR) technology in Bokor field, Sarawak, *SPE*, **72125**, 2001, 1-12.
- [6] Li, J., Liu, J., Trefry, M.G., Park, J., Liu, K., Haq, B., Johnston, C.D., VolK, H., Interactions of microbial enhanced oil recovery processes, submitted to *Transport in Porous Media*.
- [7] Li, Q., Kang, C., Wang, H., Liu, C. & Zhang, C., Application of microbial enhanced oil recovery technique to Daqing oilfield, *Biochem. Eng. J.*, **11**, 2002, 197-199.
- [8] Li, Y., Abriola, L.M., Phelan, T.J., Ramsburg, C.A. & Pennell, K.D., Experimental and numerical validation of the total trapping number for prediction of DNAPL mobilization, *Environ. Sci. Technol.*, **41**, 2007, 8135-8141.
- [9] Pennell, K.D., Pope, G.A. & Abriola, L.M., Influence of viscous and buoyancy forces on the mobilization of residual tetrachloroethylene during surfactant flushing, *Environ. Sci. Technol.*, **30**, 1996, 1328-1335.
- [10] Zhang, X., Knapp, R.M. & McInerney, M.J., A mathematical model for microbially enhanced oil recovery process, *SPE/DOE*, **24202**, 1992, 469-479.